International Journal of GEOMATE, Oct., 2024 Vol.27, Issue 122, pp. 104-114
ISSN: 2186-2982 (P), 2186-2990 (O), Japan, DOI: https://doi.org/10.21660/2024.122.4559
Geotechnique, Construction Materials and Environment

FATIGUE LIFE AND SUSTAINABILITY OF POLYPROPYLENE FIBER-REINFORCED CONCRETE FOR CONCRETE PAVEMENT

*Tsuneji Sasaki[1], Hiroshi Higashiyama[2] and Mutsumi Mizukoshi[3]

[1]Okumura Engineering Corporation, Japan; [2]Department of Civil and Environmental Engineering, Kindai University, Japan; [3]Department of Civil Engineering, Kobe City College of Technology, Japan

*Corresponding Author, Received: 22 May 2024, Revised: 11 Sep. 2024, Accepted: 16 Sep. 2024

ABSTRACT: This paper presents the fatigue properties of polypropylene fiber-reinforced concrete (PPFRC) in flexure at various stress ratios and the sustainability of PPFRC in terms of environmental impact and material cost for jointed concrete pavements. In this study, prism specimens with a size of 100 × 100 × 400 mm were cut from slabs with a size of 1000 × 1000 × 100 mm, considering the effects of fiber distribution and orientation. A polypropylene fiber with a size of 0.7 × 30 mm was mixed into concrete at 1.0 and 1.3 vol.%. Fatigue tests were conducted under four-point flexural loading to obtain the S-N curve for each mixture. In this study, plain concrete (PLC20) with a maximum aggregate size of 20 mm was also used, and its fatigue strength was compared with that of the PPFRCs. Based on the fatigue test results, the S-N curves called the Whöler curve were proposed. The fatigue life of the 1.3 vol.% PPFRC was longer than that of PLC20 at a lower stress ratio. Using the obtained S-N curves, a jointed concrete pavement was designed. The fatigue life of the thinner PPFRC with 1.3 vol.% pavement was enhanced significantly compared with a normal jointed concrete pavement. Consequently, despite the higher initial material cost, the 1.3 vol.% PPFRC can reduce pavement thickness and CO_2 emissions.

Keywords: Polypropylene fiber-reinforced concrete pavement, Fly ash, Fatigue life, CO_2 emissions, Material cost

1. INTRODUCTION

Concrete pavements (rigid pavements) require less maintenance and less life-cycle cost than asphalt pavements (flexural pavements) [1]. However, concrete pavements have a longer curing period of concrete and a higher initial cost than asphalt pavements [1]. Regarding the environmental impacts, cement production emits high carbon dioxide (CO_2) [2, 3]. To reduce CO_2 emissions from cement production and to enhance the sustainability of concrete pavements, researchers and engineers have investigated the utilization of alternative cementitious materials and recycled materials [4-8], the reduction of pavement thickness, the enhancement of fatigue life using fiber-reinforced concretes (FRCs) [9-13], and the economic and environmental impacts of concrete pavements [14-17].

Generally, adding steel and other fibers into concrete improves fatigue performance and reduces crack growth depending on the fiber type and geometry, fiber content, and fiber distribution [18]. Although many researchers have studied the fatigue characteristics of steel fiber-reinforced concrete (SFRC) [19-27], the studies on the fatigue performance of polypropylene fiber-reinforced concrete (PPFRC) in flexure are limited in the literature [28, 29]. Polypropylene fibers are less costly and have higher elongation than other synthetic fibers without corrosion. Tawfiq et al. [28] investigated the flexural fatigue performance of PPFRC using two geometries of polypropylene (PP) fibers, such as monofilament and collated fibrillated fibers, with different fiber volume fractions. They prepared prism specimens with and without single-edge small notches, and the fatigue test results showed the extension of the crack initiation and propagation periods. Mizoguchi et al. [29] used two types of PP fibers such as split yarn and emboss texture, with a fiber volume fraction of 1.0%. Their fatigue test results revealed the enhanced fatigue life of the PPFRC in comparison with plain concrete.

The mechanical properties of fiber-reinforced concrete are affected by the fiber distribution and orientation [30-33]. Large-scale structures such as pavements and slabs are less susceptible to the wall effect than the standard prism specimens. In the previous study by the authors [34], the mechanical properties of PPFRC under static flexural loading were compared between specimens prepared with different methods, one prepared as per the standard specification [35], and others prepared by cutting prism specimens from large-size slabs. The post-cracking behavior of prism specimens from large-size slabs significantly decreased in comparison with the standard prism specimens due to the fiber distribution and orientation [34, 36].

The aims of this study are to obtain the fatigue strength of PPFRCs with two fiber volume fractions of 1.0 and 1.3% for the fatigue design of PPFRC pavements and to compare the fatigue life of PPFRC pavements with that of a normal jointed concrete pavement as per the design methodology [37]. In the construction sector, lesser use of cement and the use

of alternative materials or supplementary cementitious materials (SCMs) leads to the reduction of CO_2 emissions [7]. In this study, fly ash (FA), which is commonly used all over the world, is employed as one of the SCMs. In terms of environmental impact and economic feasibility, the CO_2 emissions and the initial material cost were also evaluated based on the fatigue design results.

2. RESEARCH SIGNIFICANCE

Concrete pavements with a long service life and low environmental impact are widely investigated and discussed throughout the world. FRCs improve the material properties of concrete, including the fatigue strength, depending on the fiber type and content. Therefore, research work on the fatigue properties of FRCs used for pavements is significantly important for performance-based design. In this study, the authors investigated the fatigue strength, CO_2 emissions, and the initial material cost of PPFRC pavements in comparison with normal jointed concrete pavements to establish sustainable concrete pavements.

3. MATERIALS AND TEST METHODS

3.1 Materials and Specimens

Ordinary Portland Cement (OPC) and FA were used as binders. The OPC has a density of 3.15 g/cm^3 and a Blaine fineness of 3270 cm^2/g. The FA has a density of 2.25 g/cm^3 and a Blaine fineness of 3780 cm^2/g, which was classified into Type II in Japan. As per the datasheet from the manufacturer [38], the PP fiber with an embossed surface texture shown in Fig. 1 has a length of 30 mm, an equivalent diameter of 0.7 mm, a tensile strength of 500 N/mm^2, Young's modulus of 8 kN/mm^2, and a density of 0.91 g/cm^3. Two kinds of fine aggregates and coarse aggregates were used for concrete in this study. The maximum aggregate size was 20 mm. The physical properties of the materials used are shown in Table 1.

The mixture proportion of plain concrete is shown in Table 2. The water-to-binder ratio (W/B) was 0.4, which was determined based on the supply for jointed concrete pavements. The FA was replaced by 20% of the cement based on the previous test results [39]. The fiber volume fractions of the PP fiber were 1.0 and 1.3%. The air-entraining agent and the high-range water-reducing agent were properly used to gain the target air content and slump, namely, the target air content of 4.5 ± 1.5% and the slump of 5.0 ± 2.5 cm after the PP fiber was added.

Square slabs with 1000 × 1000 × 100 mm, shown in Fig. 2, were prepared for the PPFRCs with fiber volume fractions of 1.0 and 1.3 vol.%. For the plain concrete with a maximum aggregate size of 20 mm (PLC20), prism specimens with 100 × 100 × 400 mm were prepared using steel molds. After casting, these prism specimens and slabs were covered with a wet damp cloth for curing at a laboratory-controlled temperature of 20 ± 2°C or cured in water tanks at a laboratory-controlled temperature of 20 ± 2°C. In general, the fiber distribution and orientation were affected in the mold size under the wall effect [30-33]. In this study, as the target was for a PPFRC pavement, the prism specimens with 100 × 100 × 400 mm were cut from the square slabs as shown in Fig. 3. After cutting, all specimens were cured in water tanks at the laboratory-controlled temperature of 20 ± 2°C until the age of 28 days. After curing until the age of 28 days, all specimens were cured in the dry condition at the laboratory-controlled temperature of 20 ± 2°C until the fatigue tests.

Fig. 1 Overview of polypropylene fiber

Table 1. Material properties

Materials	Type	Sign	Properties
Cement	Portland cement	C	Density: 3.15 g/cm^3
Fly ash	Second class	FA	Density: 2.25 g/cm^3
Fine aggregate	Sea sand	S1	Density: 2.57 g/cm^3 (saturated surface-dry condition)
	Crushed sand	S2	Density: 2.67 g/cm^3 (saturated surface-dry condition)
Coarse aggregate	Crushed stone	G	Density: 2.69 g/cm^3 (saturated surface-dry condition) G_{max}:20mm
Admixture	High-range water-reducing agent	SP	Polycarboxylic acid type
	Air-entraining agent	AE	Surface active agent of higher acids
Fiber	Polypropylene fiber	PP	Diameter: 700 μm Length: 30 mm Density: 0.91 g/cm^3 Tensile strength: 500 N/mm^2 Young's modulus: 8 kN/mm^2

Table 2. Mixture proportion of plain concrete

W/B (%)	s/a (%)	FA (%)			
40	50	20			
Unit content (kg/m^3)					
W	C	FA	S1	S2	G
165	330	83	425	424	872

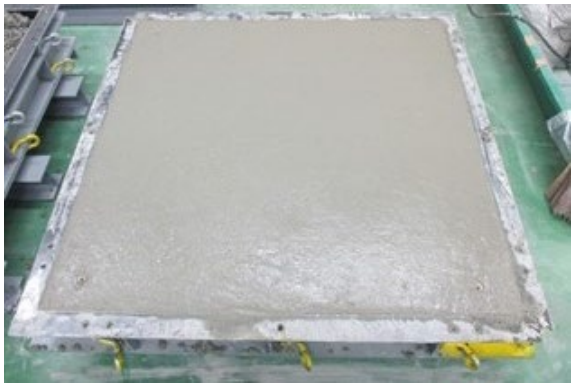

Fig. 2 PPFRC casting into a square slab mold

Fig. 3 Prism specimens cut from the square slab

3.2 Test methods

3.2.1 Flexural static tests

The four-point flexural static tests shown in Fig. 4 were carried out to determine a fatigue load using two or three prism specimens as per JSCE-G 552-2013 [40] when each flexural fatigue test was started. In the flexural static tests, the constant loading rate of 0.1 mm/min was maintained.

3.2.2 Flexural fatigue tests

The four-point flexural fatigue tests were conducted using a servo-hydraulic testing machine as shown in Fig. 5. The span length was 300 mm. The minimum load of 2 kN was applied at all stress ratios. The stress ratio is the applied flexural stress at the bottom surface of a specimen divided by the flexural static strength (modulus of rapture: MOR). The applied maximum load was determined based on the flexural static strength at each stress ratio. The loading speed was maintained at 5 Hz and the loading wave type was a sinusoidal wave.

4. RESULTS AND ANALYSIS

4.1 Flexural static strength

The flexural static strength at the start of each set of fatigue tests is listed with the curing age in Table 3. The relationship between the flexural static strength and the compressive strength as per JIS A 1108 [41], including the results in the previous study [34, 36, 39] is shown in Fig. 6. The flexural static strength is almost as per the following equation proposed for PLC by Noguchi and Tomosawa [42]:

$$f_r = 0.440 {f_c'}^{0.678} \quad (1)$$

where f_r is the flexural static strength (MOR) (N/mm^2) and f'_c is the compressive strength (N/mm^2).

These results show that the PP fiber content is not expected to increase the flexural static strength of PPFRC due to its lower Young's modulus as shown in Table 1.

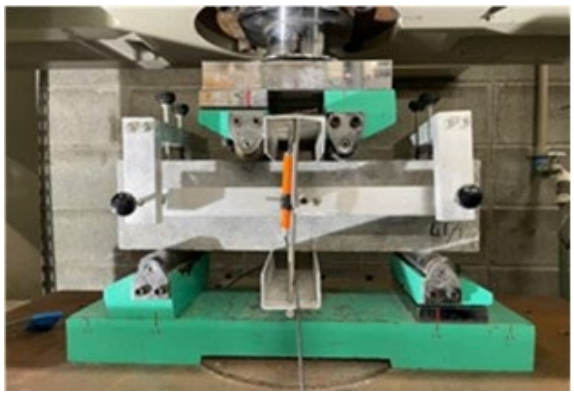

Fig. 4 Four-point flexural static test setup

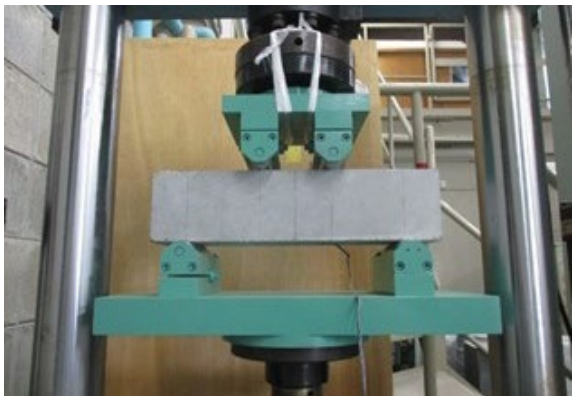

Fig. 5 Four-point flexural fatigue test setup

Table 3. Results of flexural static tests

PLC20		1.0 vol.% PPFRC		1.3 vol.% PPFRC	
Flexural static strength (N/mm^2)	Curing age (days)	Flexural static strength (N/mm^2)	Curing age (days)	Flexural static strength (N/mm^2)	Curing age (days)
I: 6.47	63	I: 6.63	143	I: 6.24	106
II: 6.31	34			II: 7.81	144
III: 5.12	57				

Table 4. Results of flexural fatigue tests

PLC20			1.0 vol.% PPFRC			1.3 vol.% PPFRC		
Stress ratio S	Fatigue life N		Stress ratio S	Fatigue life N		Stress ratio S	Fatigue life N	
0.85	2,241	III	0.80	118	I	0.85	410	I
	2,853	III		674	I		815	I
	4,369	III		3,308	I	0.80	6,322	II
0.80	3,377	I		10,866	I		15,308	II
	26,700	I	0.75	365	I		30,780	II
	30,797	I		16,729	I		55,581	II
	56,416	I		30,940	I	0.77	399,533	I
0.75	44,572	I		141,878	I		435,477	I
	70,076	II		186,900	I		539,229	I
	105,453	I	0.70	10,435	I	0.75	105,846	II
	160,340	I		161,866	I		209,034	II
				2,196,724	I		231,720	II
				3,766,345	I		337,105	I
						0.71	1,526,107	I

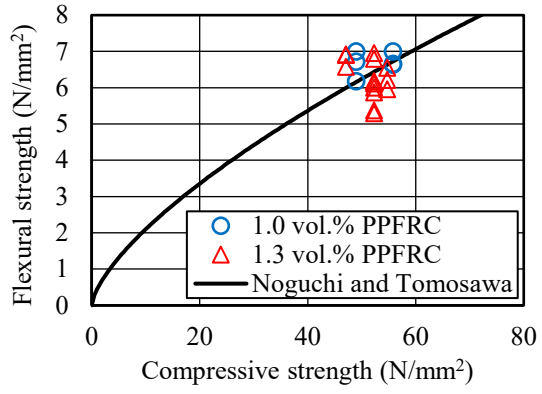

Fig. 6 Flexural strength vs. compressive strength

4.2 Flexural fatigue properties

4.2.1 Probabilistic analysis

In general, the reliability against the fatigue failure is analyzed to use an adequate mathematical model. In this study, for the simplicity and practicability, the logarithmic normal distribution was used to assess the S-N curves. The probability of survival can be determined by the following equation:

$$P_s = 1 - \frac{1}{n+1} \quad (2)$$

where P_s is the probability of survival; i is the failure order number; and n is the number of fatigue data sets for a given stress ratio.

The logarithmic normal distribution model can be expressed by the following equation:

$$t = AlogN + B \quad (3)$$

where t is the standard normally distributed variable; N is the fatigue life; and A and B are the experimental coefficients.

The stress ratio (S) and the fatigue life (N) of all specimens were summarized in Table 4. For each stress ratio in each mixture, the probabilities of survival (standard normally distributed variables) are plotted against the fatigue lives, and each linear regression line is obtained as shown in Fig. 7. The wider variation can be seen for the 1.0 vol.% PPFRC in comparison with the other mixtures. The lower amount of PP fiber might cause a wider variation in the fatigue life. However, this characteristic of PPFRC under the flexural fatigue is yet to be revealed in this study. Further fatigue tests are thus needed to understand the fatigue properties of PPFRC with a lower fiber content.

4.2.2 S-N curves

The S-N curve as the Whöler curve for each mixture can be expressed using the following equation:

$$logN = -aS + b \quad (4)$$

where N is the fatigue life; S is the stress ratio; and a and b are the experimental coefficients.

The S-N curve of PLC20 having the probability of survival at 0.5 is shown in Fig. 8(a) and given as the following equation:

$$logN = -14.488S + 15.827 \quad (5)$$

The S-N curve proposed by Banjara et al. [43] is also shown in Fig. 8(a). The fatigue test results in this study agree well with their S-N curve presented as the following equation:

$$logN = -12.887S + 14.521 \quad (6)$$

The S-N curves of the 1.0 vol.% PPFRC and the 1.3 vol.% PPFRC having the probability of survival at 0.5 are respectively shown in Fig. 8(b) and (c) together with the curves of PLC20 and Banjara et al.

[43]. At higher stress ratios, the fatigue lives of the PPFRCs, especially the 1.0 vol.% PPFRC, decrease in comparison with that of PLC20. However, the fatigue life of the 1.3 vol.% PPFRC is enhanced under the stress ratio of 0.8. Here, the 1.0 vol.% PPFRC is not considered as a concrete pavement option due to its lower fatigue strength at this stage for the reason mentioned above.

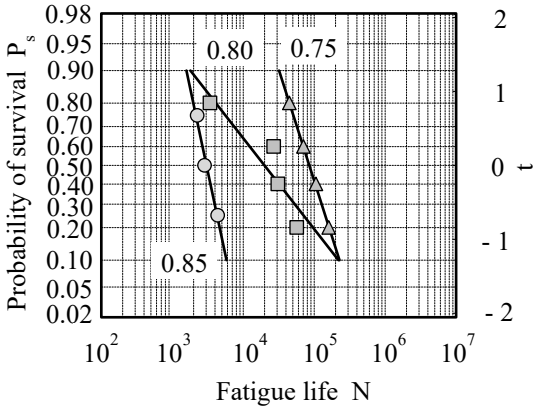

(a) PLC20

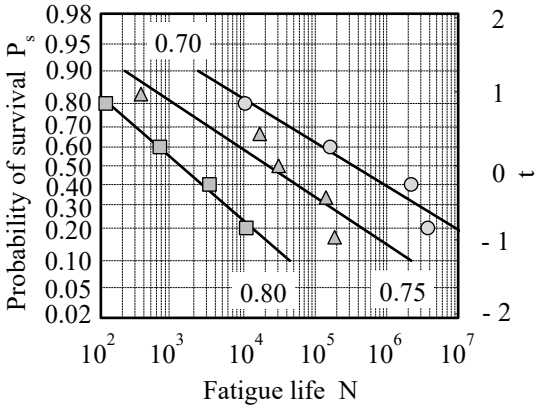

(b) 1.0 vol.% PPFRC

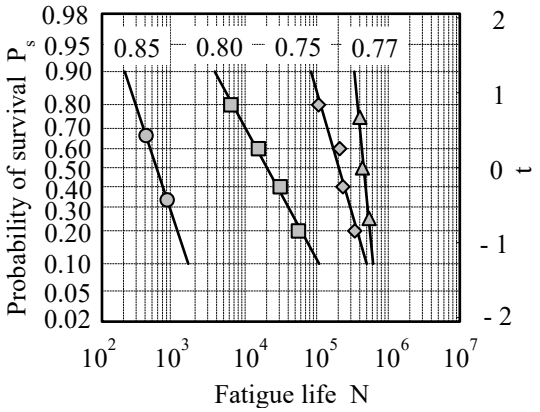

(c) 1.3 vol.% PPFRC

Fig. 7 Probability of survival vs. fatigue life

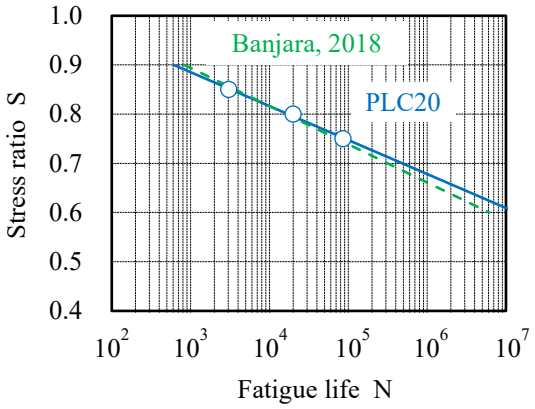

(a) PLC20

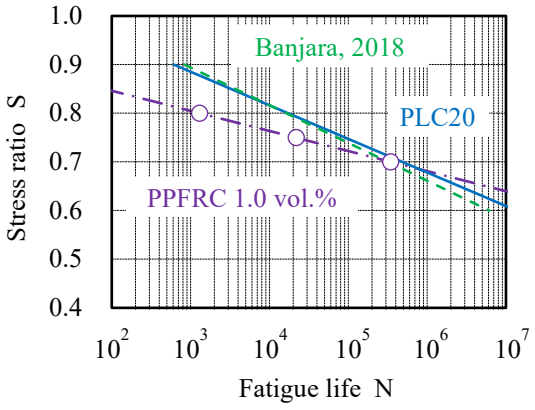

(b) 1.0 vol.% PPFRC

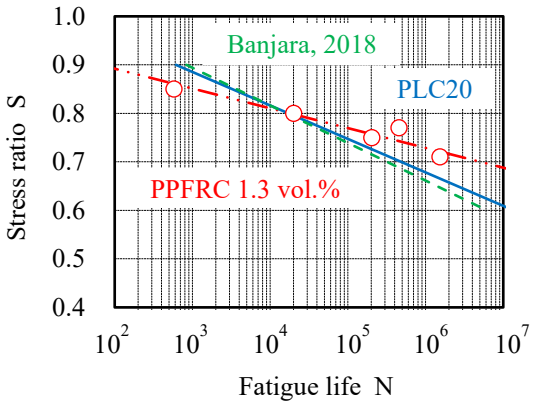

(c) 1.3 vol.% PPFRC

Fig. 8 S-N curves

The S-N curve of the 1.3 vol.% PPFRC having the probability of survival at 0.5 is given as the following equation:

1.3 vol.% PPFRC

$$logN = -24.498S + 23.854 \quad (7)$$

4.2.3 Design S-N curves

Regarding the performance-based design, the coefficients of a and b in Eq. (4) are better given as a function of the probability of survival [44]. From the results shown in Fig. 7, the coefficients of a and b ranging from 0.5 to 0.95 of the probability of survival (P_s) for each mixture are shown in Fig. 9. Each coefficient can be accurately represented by the quadratic equations as follows:

PLC20

$$a = -4.9705P_s^2 + 3.3027P_s + 14.052 \quad (8)$$

$$b = -6.0175P_s^2 + 4.0111P_s + 15.293 \quad (9)$$

1.3 vol.% PPFRC

$$a = -38.376P_s^2 + 67.939P_s + 0.743 \quad (10)$$

$$b = -32.596P_s^2 + 55.964P_s + 4.516 \quad (11)$$

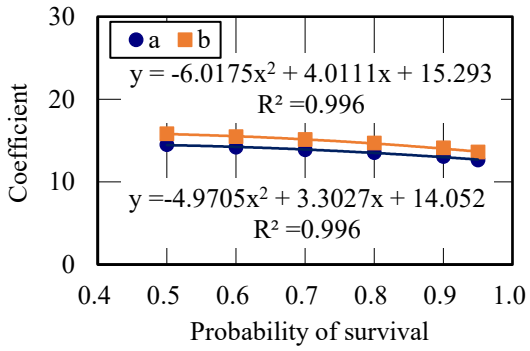

(a) PLC20

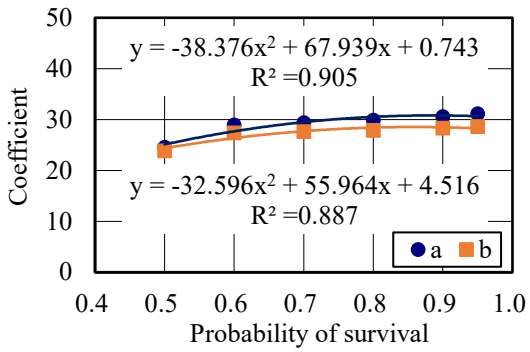

(b) 1.3 vol.% PPFRC

Fig. 9 Coefficients for S-N curves

5. FATIGUE LIFE OF PPFRC PAVEMENT

Using example design conditions and the design methodology for jointed concrete pavements provided in [37], the fatigue lives of 1.3 vol.% PPFRC pavement and PLC20 pavement were calculated as per [37]. Their cross-sectional layered view is shown in Fig. 10. The design conditions for the base, subgrade, traffic volume, temperature difference, and others are summarized in Tables 5 to 9. The S-N curves having the probability of survival of 0.9 were determined using Eq. (8) to Eq. (11) in this calculation. The pavement thickness was varied from 21 cm to 30 cm in units of 1 cm. Here, the characteristic flexural strength of concrete was fixed to 6.4 N/mm^2 that is assumed to be obtained by using prism specimens of 100 × 100 × 400 mm. Then, considering the coefficient of variation of 16%, the design flexural strength was 5.3 N/mm^2. It was also assumed that dowel bars and tie bars are arranged in the transverse and longitudinal joints for all pavements. Furthermore, the previous study [34] confirms that the size effect of flexural static strength of the 1.3 vol.% PPFRC can be determined as per the following equation proposed for PLC by Yoshimoto et al. [44]:

$$f_{r,h} = 0.43\left(1 + \frac{7.04}{\sqrt[3]{h}}\right) f_{r,150} \quad (12)$$

where $f_{r,h}$ is the flexural static strength (N/mm^2) of the specimen height of h (mm) and $f_{r,150}$ is the flexural static strength (N/mm^2) of the specimen height of 150 mm.

The results of fatigue life prediction based on cumulative fatigue damage are shown in Table 10. The 1.3 vol.% PPFRC can significantly enhance the fatigue life and reduce the pavement thickness when compared with the PLC20 in this study. The standard design life of 20 years can be satisfied with a thickness of 27 cm for the PLC20 and with a thickness of 24 cm for 1.3 vol.% PPFRC. However, to achieve the sustainable concrete pavements, the longer design life ranging from 30 to 60 years should be considered [45]. When the target design life is set to 60 years, as shown in Table 10, the PLC20 and the 1.3 vol.% PPFRC can be accomplished with thicknesses of 28 cm and 25 cm, respectively. Then, the thickness of the 1.3 vol.% PPFRC is reduced by about 11% as compared with PLC20.

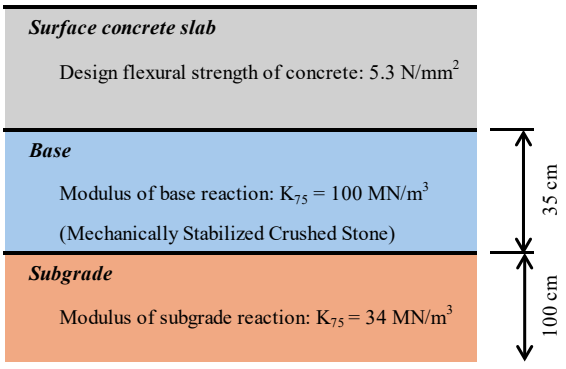

Fig. 10 Cross-sectional layered view

Table 5. Example of design conditions

Items	Design conditions
One-way daily traffic volume of heavy vehicles	1,000 to 2,999
Repetitive number of wheel loads	Table 6
Cracking density	10 cm/m^2
Degree of reliability	90%
Characteristic flexural strength of concrete	6.4 N/mm^2
Design flexural strength of concrete	5.3 N/mm^2
Young's modulus of concrete	34,000 N/mm^2
Poisson's ratio	0.2
Coefficient of thermal expansion	10×10^{-6}/℃
Position of running wheel loads	Table 7
Ratio of heavy vehicles	Table 8
Modulus of subgrade reaction	K_{75} = 34 MN/m^3
Modulus of base reaction	K_{75} = 100 MN/m^3
Frequency of temperature difference of pavement	Table 9
Transverse joint interval	10 m
Number of lanes	4
Width of a lane	3.25 m

Table 6. Repetitive number of wheel loads [37]

Wheel load (kN)	Daily traffic volume
9.8	9,998
19.6	2,418
29.4	1,802
39.2	980
49.0	505
58.8	329
68.6	182
78.4	81
88.2	36
98.0	19

Table 7. Position of running wheel loads [37]

Position of running wheel load (cm)	Frequency
15	0.05
45	0.10
75	0.25
105	0.20

Table 8. Ratio of heavy vehicles [37]

Positive temperature difference	Negative temperature difference
0.6	0.4

Table 9. Frequency of temperature difference of pavement [37]

Classification of temperature difference (℃)	Frequency of small temperature difference		
Thickness (cm)	25	28	30
19	0	0	0
17	0	0	0
15	0.002	0.004	0.007
13	0.016	0.021	0.025
11	0.037	0.045	0.053
9	0.085	0.080	0.080
7	0.110	0.110	0.115
5	0.155	0.150	0.140
3	0.205	0.210	0.210
-1	0.390	0.380	0.370
1	0.600	0.530	0.480
-3	0.335	0.360	0.380
-5	0.063	0.100	0.120
-7	0.002	0.010	0.020
-9	0	0	0

6. CO_2 EMISSIONS AND MATERIAL COST

As the authors mentioned in the previous study [34], the reduced pavement thickness and the use of FA contribute to reducing CO_2 emissions by reducing the amount of cement used. However, the addition of PP fiber increases the material cost. Furthermore, the PP fiber has relatively higher CO_2 emission intensity as shown in Table 11. Based on the pavement thickness results shown in Chapter 5, the amount of CO_2 emissions per year during the design life of 60 years associated with the production of materials with PLC20 and 1.3 vol.% PPFRC is estimated. Here, in normal jointed concrete pavements, a steel mesh [46] is usually installed into concrete to prevent cracks and restrain the crack width. In contrast, as the PP fiber is expected to suppress the crack width, a steel mesh is not used for the 1.3 vol.% PPFRC pavement. Elimination of the steel mesh is advantageous to reduce CO_2 emissions and the material cost, and to efficiently construct jointed concrete pavements. The CO_2 emission intensity for each material referred to in the literatures [2, 47-50] is shown in Table 11.

Fig. 11 shows the estimated CO_2 emissions associated with material production for PLC20 and for 1.3 vol.% PPFRC per year during the design life of 60 years. The pavement thicknesses of PLC20 and 1.3 vol.% PPFRC are 28 cm and 25 cm for a design life of 60 years, respectively. PLC20 was prepared in two formulations, one with only OPC as the binder (PLC20_FA0) and the other with 20% of the OPC replaced with FA (PLC20_FA20). The estimation

results show 1.57 kg-CO_2/m^2/year for PLC20_FA0, 1.28 kg-CO_2/m^2/year for PLC20_FA20, and 1.20 kg-CO_2/m^2/year for 1.3 vol.% PPFRC. The 1.3 vol.% PPFRC emits the lowest amount of CO_2. Then, the CO_2 emission of 1.3 vol.% PPFRC is reduced by about 24% for PLC20_FA0 and 7% for PLC20_FA20. The partial replacement of OPC with the FA is effective to reduce CO_2 emissions, and the PP fiber addition contributes largely to enhance the fatigue life of concrete pavements.

Table 10. Results of fatigue life prediction

Thickness (cm)	Fatigue life (years)	
	PLC20	1.3 vol.% PPFRC
21	-	-
22	-	2
23	-	11
24	-	23
25	5	82
26	14	489
27	29	-
28	149	-
29	201	-
30	-	-

Table 11. CO_2 emission intensity

Materials	CO_2 emission (kg-CO_2/t)
Portland cement	788.6
Fly ash	17.9
Fine aggregate	3.5
Coarse aggregate	2.8
PP fiber	1785.0
Steel	755.0

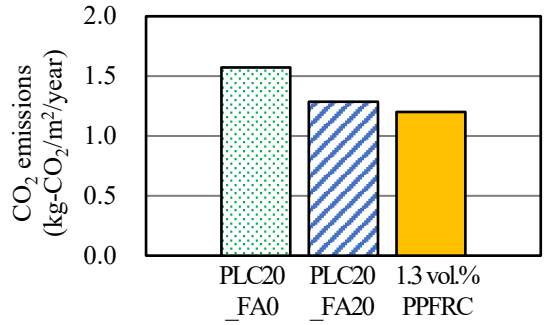

Fig. 11 CO_2 emissions

Next, we calculated their initial material cost. The unit cost of each mixture is shown in Table 12. Fig. 12 shows the calculated initial material cost required by each mixture to satisfy the design life of 60 years. The results show 9,832 JPY/m^2 for PLC20_FA0, 9,972 JPY/m^2 for PLC20_FA20, and 12,311 JPY/m^2 for 1.3 vol.% PPFRC. The initial material cost of 1.3 vol.% PPFRC pavement was 23% higher than that of PLC20 pavement due to the PP fiber addition. In this study, only the initial material cost was used for comparison. However, because the steel mesh is not used in the 1.3 vol.% PPFRC pavement, the construction days and the total construction cost required might be decreased depending on the construction volume, and the cost difference may be smaller. In the future study, the life-cycle cost and CO_2 emissions including material production, construction, maintenance and preservation, and end-of-life will be used for comparison.

Table 12. Unit cost of each mixture

Mixtures	Unit cost
Ready-mixed concrete PLC20_FA0	31,400 JPY/m^3
Ready-mixed concrete PLC20_FA20	31,900 JPY/m^3
Ready-mixed concrete 1.3 vol.% PPFRC	49,245 JPY/m^3
Steel mesh	1,040 JPY/m^2

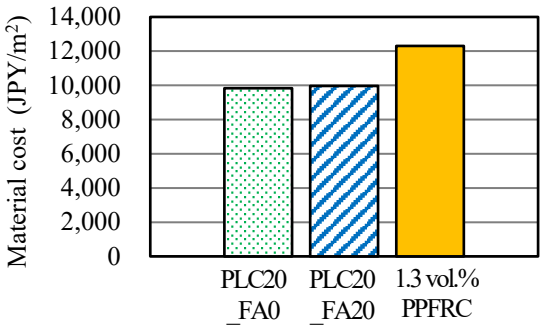

Fig. 12 Initial material cost for a design life of 60 years

7. CONCLUSIONS

In this study, the fatigue strength of two types of PPFRC with fiber volume fractions of 1.0 and 1.3%, and PLC20 was determined for the fatigue design of pavements. The fatigue life of 1.3 vol.% PPFRC pavement was compared with that of normal jointed concrete pavements. Furthermore, the reduction of CO_2 emissions and the reduction of material cost were estimated based on the fatigue design results. The findings are as follows:

(1) For the survival probability of 0.5, the fatigue life of 1.3 vol.% PPFRC is longer than that of PLC20

as the stress ratio decreases. Based on the fatigue test results, the S-N curve was proposed for the design of 1.3 vol.% PPFRC pavement.

(2) The addition of PP fiber at 1.3 vol.% leads to a longer fatigue life of concrete pavement. The 1.3 vol.% PPFRC pavement can also reduce the pavement thickness compared with PLC20 pavement. When the target design life is set to 60 years, the PLC20 with a thickness of 28 cm and the 1.3 vol.% PPFRC with a thickness of 25 cm can be accomplished. The thickness of the 1.3 vol.% PPFRC is reduced by about 11% compared with PLC20.

(3) Comparing the CO_2 emissions associated with material production for PLC20 and 1.3 vol.% PPFRC per year during the design life of 60 years, 1.3 vol.% PPFRC can reduce CO_2 emissions by about 24%.

(4) Comparing the initial material costs of PLC20 and 1.3 vol.% PPFRC having the design life of 60 years, the initial material cost of 1.3 vol.% PPFRC was about 23% higher due to the fiber addition. However, as the steel mesh is not used in the 1.3 vol.% PPFRC pavement, the construction days and the costs required might be decreased. Furthermore, the cost difference can be smaller when the total life-cycle cost is included.

8. ACKNOWLEDGMENT

The authors would like to express the sincere appreciation for the financing of a part of this research by Research Committee on Technological Development for Infrastructure, Osaka, Japan.

9. REFERENCES

[1] Pavement Committee, Design and Construction of Pavement Sub-committee, Guidebook for concrete pavement 2016, Japan Road Association, 2016, pp. 1-336 (in Japanese).

[2] Japan Cement Association, LCI data of Cement 2023, https://www.jcassoc.or.jp/cement/4pdf/jg1i_01.pdf (accessed Dec. 26, 2023).

[3] Kirino, Y., Shinmi, T., Kawai, K., and Itsubo, N., Environmental impact assessment of world cements considering production method and environmental condition in each country, Cement Science and Technology, Vol. 73, 2020, pp. 401-406 (in Japanese).

[4] Yener, E. and Hinislioğlu, S., The effects of silica fume and fly ash on the scaling resistance and flexural strength of pavement concretes, Road Materials and Pavement Design, Vol. 12, No. 1, 2011, pp. 177-194.

[5] Shinmi, T., Yamate, T., Fuji, Y., and Kawai, K., Properties and CO_2 emission of pavement concrete based on blended cement, Cement Science and Technology, Vol. 68, 2015, pp. 283-290 (in Japanese).

[6] Yoshitake, I., Ueno, S., Ushio, Y., Arano, H., and Fukumoto, S., Abrasion and skid resistance of recyclable fly ash concrete pavement made with limestone aggregate, Construction and Building Materials, Vol. 112, 2016, pp. 440-446.

[7] Pranav, S., Aggarwal, S., Yang, E. H., Sarkar, A. K., Singh, A. P., and Lahoti, M., Alternative materials for wearing course of concrete pavements: A critical review, Construction and Building Materials, Vol. 236, 2020, 117609.

[8] Talkeri, A., Shankar, A. U. R., Alkali activated slag-fly ash concrete incorporating precious slag as fine aggregate for rigid pavements, Journal of Traffic and Transportation Engineering, Vol. 9, No. 1, 2022 pp. 78-92.

[9] Roesler, J. R., Lange, D. A., Altoubat, S. A., Rieder, K. A., and Ulreich, G. R., Fracture of plain and fiber-reinforced concrete slabs under monotonic loading, ASCE, Journal of Materials in Civil Engineering, Vol. 16, No. 5, 2004, pp. 452-460.

[10] Meda, A. and Plizzari, G. A., New design approach for Steel fiber-reinforced concrete slabs-on-ground based on fracture mechanics, ACI Structural Journal, Vol. 101, No. 3, 2004, pp. 298-303.

[11] Altoubat, S. A., Roesler, J. R., Lange, D. A., and Rieder, K. A., Simplified method for concrete pavement design with discrete structural fibers, Construction and Building Materials, Vol. 22, 2008, pp. 384-393.

[12] Nayar, S. K. and Gettu, R., A comprehensive methodology for the design of fiber-reinforced concrete pavements, FRC 2014 Joint ACI-fib International Workshop Fiber-Reinforced Concrete: From Design to Structural Applications, 2014, pp. 321-330.

[13] Ozturk, O., Ozyurt, N., Sustainability and cost-effectiveness of steel and polypropylene fiber reinforced concrete pavement mixtures, Journal of Cleaner Production, Vol. 363, 2022, 132582.

[14] Ali, B., Qureshi, L. A., and Kurda, R., Environmental and economic benefits of steel, glass, and polypropylene fiber reinforced cement composite application in jointed plain concrete pavement, Composites Communications, Vol. 22, 2020, 100437.

[15] Ozturk, O. and Ozyurt, N., Sustainability and cost-effectiveness of steel and polypropylene fiber reinforced concrete pavement mixtures, Journal of Cleaner Production, Vol. 363, 2022, 132582.

[16] Ali, B., Ahmed, H., Hafez, H., Brahmia, A., El Ouni, M. H., and Raza, A., Life cycle assessment (cradle-to-gate) of fiber-reinforced concrete application for pavement use: A case study of Islamabad city, International Journal of Pavement

Research and Technology, Vol. 16, 2023, pp. 247-263.
[17] Patil, R. R. and Katare, V. D., Application of fiber reinforced cement composites in rigid pavements: A review, Materials Today: Proceedings, Available online May 10, 2023.
[18] Johnston, C. D. and Zemp, R. W., Flexural fatigue performance of steel fiber reinforced concrete -influence of fiber content, aspect ratio, and type, ACI Materials Journal, Vol. 88, No. 4, 1991, pp. 374-383.
[19] Baston, G., Ball, C., Bailey, L., Lenders, E., and Hooks, J., Flexural fatigue strength of steel fiber reinforced concrete beams, ACI Journal, Proceedings, Vol. 69, No. 11, 1972, pp. 673-677.
[20] Ibuki, S., Kokubu, S., and Oshima, T., Flexural fatigue of steel fiber reinforced concrete, Proceedings of the Japan Concrete Institute, Vol. 1, 1979, pp. 421-424 (in Japanese).
[21] Ramakrishnan, V. Oberling, G., and Tatnal, P., Flexural fatigue strength of steel fiber concrete, Fiber reinforced concrete-Properties and applications, SP-105-13, ACI Special Publication, 1987, pp. 225-245.
[22] Otter, D. E. and Naaman, A. E., Properties of steel fiber reinforced concrete under cyclic load, ACI Materials Journal, Vol. 85, No. 4, 1988, pp. 254-261.
[23] Mizukoshi, M., Shimauchi, H., Kakuma, F., and Matsui, S., Flexural fatigue characteristics of steel fiber reinforced concrete, Proceedings of the Japan Concrete Institute, Vol. 16, No. 1, 1994, pp. 1055-1060 (in Japanese).
[24] Zhang, J. and Stang, H., Fatigue performance in flexure of fiber reinforced concrete, ACI Materials Journal, Vol. 95, No. 1, 1998, pp. 58-67.
[25] Zhang, J., Stang, H., and Li, V. C., Fatigue life prediction of fiber reinforced concrete under flexural load, International Journal of Fatigue, Vol. 21, 1999, pp. 1033-1049.
[26] Lee, M. K. and Barr, B. I. G., An overview of the fatigue behavior of plain and fiber reinforced concrete, Cement & Concrete Composites, Vol. 26, 2004, pp. 299-305.
[27] Singh, S. P., Singh, B., and Kaushik, S. K., Probability of fatigue failure of steel fibrous concrete, Magazine of Concrete Research, Vol. 57, No.2, 2005, pp.65-72.
[28] Tawfiq, K., Amaghani, J., and Ruiz, R., Fatigue cracking of polypropylene fiber reinforced concrete, ACI Materials Journal, Vol. 96, No. 2, 1999, pp. 226-233.
[29] Mizoguchi, T., Shimoda, S., Matsuda, M., and Urano, T., An experimental study on bending fatigue properties of concrete using organic short fiber, Cement Science and Concrete Technology, Vol. 74, 2020, pp. 281-286 (in Japanese).
[30] Kobayashi, K. and Mutsuyoshi, H., Influence of fiber orientation and distribution on load-deformation characteristics of steel fiber reinforced concrete members, Proceedings of the Japan Society of Civil Engineers, Vol. 299, 1980, pp. 101-112 (in Japanese).
[31] Soroushian, P. and Lee, C. D., Distribution and orientation of fibers in steel fiber reinforced concrete, ACI Materials Journal, Vol. 87, No.5, 1990, pp. 433-439.
[32] Dupont, D. and Vandewalle, L., Distribution of steel fibers in rectangular sections, Cement & Concrete Composites, Vol. 27, 2005, pp. 391-398.
[33] Gettu, R., Gardner, D. R., Saldívar, H., and Barragán, B. E., Study of the distribution and orientation of fibers in SFRC specimens, Materials and Structures, Vol. 38, No. 1, 2005, pp. 31-37.
[34] Sasaki, T., Higashiyama, H., and Mizukoshi, M., Flexural behavior and benefits of polypropylene fiber-reinforced concrete for concrete pavement, ACI Materials Journal, Vol. 120, No. 1, 2023, pp. 219-229.
[35] JSCE-F 552-2013, Method of making specimens for strength and toughness of steel fiber reinforced concrete, Standard Specifications for Concrete Structures, Test Methods and Specifications-JSCE Standards, Japan Society of Civil Engineers, 2018, pp. 1-1756 (in Japanese).
[36] Sasaki, T., Higashiyama, H., Mizukoshi, M., Fujimori, A., and Takahara, R., Flexural properties of polypropylene fiber reinforced concrete containing fly ash for normal concrete pavement, Proceedings of International Structural Engineering and Construction, Edited by Karatas, A., Iranmanesh, A., Gurgun, A., Yazdani, S., and Singh, A., 2023, pp. MAT-02-1-MAT-02-6.
[37] Japan Road Association, Handbook for Pavement Design, 2006, pp. 1-316 (in Japanese).
[38] BarChip Inc., Products Data, https://www.barc-hip.co.jp/business/ (accessed Dec. 26, 2023).
[39] Sasaki, T., Higashiyama, H., Mizukoshi, M., and Fujimori, A., Fundamental study on concrete pavement using polypropylene fiber and fly ash, Journal of the Society of Materials Science, Japan, Vol. 72, No. 2, 2023, pp. 131-138 (in Japanese).
[40] JSCE-G 552-2013, Test method for bending strength and bending toughness of steel fiber reinforced concrete, Standard Specifications for Concrete Structures, Test Methods and Specifications, JSCE Standards, Japan Society of Civil Engineers, 2018, pp. 1-1756 (in Japanese).
[41] JIS A 1108, Method of test for compressive strength of concrete, Japan Industrial Standard, 2018, pp. 1-17.
[42] Noguchi, T. and Tomosawa, F., Relationship between compressive strength and various mechanical properties of high strength concrete, Journal of Structural and Construction Engineering, Architectural Institute of Japan, No. 472, 1995, pp. 11-16 (in Japanese).

[43] Banjara, N. K. and Ramanjaneyulu, K., Experimental investigations and numerical simulations on the flexural fatigue behavior of plain and fiber-reinforced concrete, Journal of Materials in Civil Engineering, Vol. 30, No. 8, 2018, 04018151.

[44] Yoshimoto, T., Kameta, S., and Sato, R., Proposal of a new design flexural fatigue curve for pavement concrete in consideration of the size effect, Journal of Japan Society of Civil Engineers, Ser. E1 (Pavement Engineering), Vol. 76, No. 1, 2020, pp. 18-35 (in Japanese).

[45] Federal Highway Administration, Towards sustainable pavement systems: A reference document, FHWA-HIF-15-002, 2015.

[46] Japan Road Association, Pavement design and construction guidelines, 2006, pp. 1-345 (in Japanese).

[47] Ootsuka, T., Effective use of fly ash to reduce CO_2 emissions, Concrete Journal, Japan, Vol. 59, No. 9, 2021, pp. 782-787 (in Japanese).

[48] Japan Society of Civil Engineers, Environmental load evaluation of concrete (Part 2), Concrete Technology Series 6, 2004, pp. 1-123 (in Japanese).

[49] Muroga, Y., Osawa, T., and Horiuchi, T., Drying Shrinkage Crack Control Technique in Concrete by Polypropylene Short Fibers for Concrete and Mortar, Concrete Journal, Japan, Vol. 61, No. 12, 2023, pp. 1059-1065 (in Japanese).

[50] Shinmi, T. and Yoshimoto, T., $LCCO_2$ of concrete pavement and asphalt pavement considering fuel consumption of heavy-duty vehicles, Journal of Japan Society of Civil Engineers, Ser. E1 (Pavement Engineering), Vol. 76, No. 2, 2020, pp. 69-76 (in Japanese).